Twofold efficiency increase in nanocrystalline-TiO_2/polymer photovoltaic devices by interfacial modification with a lithium salt

D. Aaron R. Barkhouse[a*], Michelle J. Carey[a], Zhibin Xie[a], Kiril R. Kirov[a], Bernard M. Henry[a], Hazel E. Assender[a], Graham R. Webster[b], Paul L. Burn[b]
[a]Department of Materials, University of Oxford, Parks Road, Oxford, UK, OX1 3PH;
[b]Department of Chemistry, University of Oxford, Chemistry Research Laboratory, Oxford University, 12 Mansfield Rd, Oxford, OX1 3TA

ABSTRACT

Modification of the interface of titanium dioxide/poly[2-(2-ethylhexyloxy)-5-methoxy-1,4,-phenylenevinylene] (TiO_2/MEH-PPV) nanocomposite photovoltaic devices with a lithium salt, $Li[CF_3SO_2]_2N$, is shown to result in a twofold increase in device efficiency. The devices are of the type ITO/TiO_2/MEH-PPV/Au. The TiO_2 layer is deposited by doctor blading a colloidal anatase paste, and the polymer is then spin-coated on top followed by thermal evaporation of gold contacts. Careful control of manufacturing conditions and use of a 35 nm polymer layer leads to a device efficiency of 0.48% for un-modified devices. The increased efficiency following Li treatment is the result of a 40% increase in both the short-circuit current and fill factor, while the open-circuit voltage remains unchanged. A maximum efficiency of 1.05% has been achieved under 80% sun illumination. This represents a record efficiency for this type of cell. Photoconductivity experiments show a substantial increase in conductivity of the TiO_2 layer following Li modification. Interfacial modification is done via a simple soaking procedure, and the effect of varying the concentration of $Li[CF_3SO_2]_2N$ is discussed. We report investigations into optimization and the mechanism of such improvement, for example by varying processing parameters of the modification procedure or the ionic species themselves.

Key words: TiO_2, polymer, MEH-PPV, nanocomposite, lithium, interface, solar cell, photovoltaic

1. INTRODUCTION

The addition of lithium and lithium salts to dye-sensitized solar cells (DSSC's) to improve photovoltaic performance has been investigated thoroughly.[1-10] Lithium has been added to liquid electrolyte DSSC's[1, 2] as well as solid-state DSSC's,[3-10] with the effects on cell performance depending on the materials combination used and the location of lithium within the device. The open-circuit voltage (V_{oc}) of devices has been reported to increase,[3-5] decrease,[1, 4] or stay the same,[2] and the short-circuit current (J_{sc}) has been shown to increase[1, 3, 5] or stay the same,[2] following treatment with lithium or a lithium salt. To date the addition of lithium to non-dye-sensitized polymer/TiO_2 solar cells has not been reported. This study looks at the effects of adding $Li[CF_3SO_2]_2N$ to MEH-PPV/TiO_2 solar cells, modifying both the polymer/TiO_2 interface and the polymer bulk, to investigate the effect of varying the concentration and location of the Li salt on device performance.

2. EXPERIMENTAL PROCEDURE

Photovoltaic devices with the structure ITO/TiO_2/MEH-PPV/Au were fabricated on patterned ITO glass. Two different types of TiO_2 layer were examined. The first was a porous TiO_2 layer produced by the doctor blading technique. Solaronix Ti-nanoxide HT (Solaronix SA, Switzerland) was spread onto the patterned ITO substrate and sintered sequentially at 100 °C for 5 minutes, 300 °C for 10 minutes, and 500 °C for 45 minutes. The resulting film was 1.2 μm thick, with an average pore size of 9-10 nm as measured by gas sorption experiments.[11] The second type of TiO_2 layer was deposited by spin coating a Ti-peroxide solution (CCIC, Japan) at 2000 rpm for 60 seconds, drying for 5 minutes at 200 °C and then sintering at 500 °C for 50 minutes. The resulting film is a smooth, dense layer approximately 50 nm

Organic Photovoltaics VII, edited by Zakya H. Kafafi, Paul A. Lane,
Proc. of SPIE Vol. 6334, 63340N, (2006) · 0277-786X/06/$15 · doi: 10.1117/12.679424

thick. The process was repeated to give a dense TiO_2 layer with an overall thickness of 100 nm. MEH-PPV, which had an average M_w = 5.4 x 10^5 and polydispersity of 20 or M_w = 2.8 x 10^5 and polydispersity of 12, was deposited by spin-coating from a chlorobenzene solution. The spin-speed and solution concentration were varied to give an MEH-PPV layer thickness of 35 - 40 nm. Au contacts were evaporated under a vacuum of ~10^{-6} mbar, to a thickness of 45 nm. The active area of each device was 6.25 mm^2.

Lithium modification of devices was done in two ways, which are termed interfacial lithium modification and polymer lithium modification. Interfacial lithium modification was done by soaking ITO/TiO_2 substrates in a solution of $Li[CF_3SO_2]_2N$ in 4 -*tert*-butyl pyridine (tBP) prior to the deposition of the polymer layer. The substrates were immersed in the solution for 20 minutes before being removed and the excess solvent blown off with a compressed air stream. The solution concentration was varied in order to vary the amount of $Li[CF_3SO_2]_2N$ adsorbed on the TiO_2 layer. Device fabrication then proceeded as described above. Polymer lithium modification was done by adding a small amount of $Li[CF_3SO_2]_2N$/tBP solution to the MEH-PPV spin-coating solution. The concentration of the $Li[CF_3SO_2]_2N$ in the spin-coating solution was varied in order to vary amount of dopant present in the resulting film.

I-V measurements of devices were done using a Keithley 2400 digital multimeter controlled by in-house software created using LabVIEW. Devices were tested under 0.8 sun AM 1.5 illumination from a Xenon arc lamp solar simulator. A 420 nm cutoff long-pass UV filter was used, and devices were mounted in an Oxford Instruments cryostat and tested under a vacuum of 10 mTorr. Unless otherwise stated, results presented are average values from at least 3 devices.

External quantum efficiency measurements were done using a CVI spectral products Xenon arc lamp, a CVI CM 110 monochromator and an Ocean Optics USB 2000 spectrometer with a cosine corrector. Devices were mounted in an Oxford instruments cryostat and tested under a vacuum of 10 mTorr.

3. RESULTS

3.1. I-V behaviour of devices

3.1.1. Mesoporous TiO_2 devices – interfacial modification

Figure 1 shows the I-V behaviour of devices with a porous TiO_2 layer made by doctor blading, with and without interfacial lithium modification. These devices were made with MEH-PPV with an average M_w = 2.8 x 10^5 and polydispersity of 12. The lithium modified devices showed substantially improved fill factors (FF) and short-circuit currents (J_{sc}), both increasing 40%. The open circuit voltage (V_{oc}) was not affected. Devices with TiO_2 layers which had been soaked in neat tBP performed identically to the control devices, so the performance enhancement cannot be attributed to tBP. The highest power conversion efficiencies (η_{max}) obtained for individual control and lithium modified devices were 0.52% and 1.05%, respectively, under 0.8 sun AM 1.5 simulated solar illumination. For the lithium modified device, this is the highest efficiency reported to date for an MEH-PPV/TiO_2 device. The remaining devices reported in this paper were made from MEH-PPV with an average M_w = 5.4 x 10^5 and polydispersity of 20.

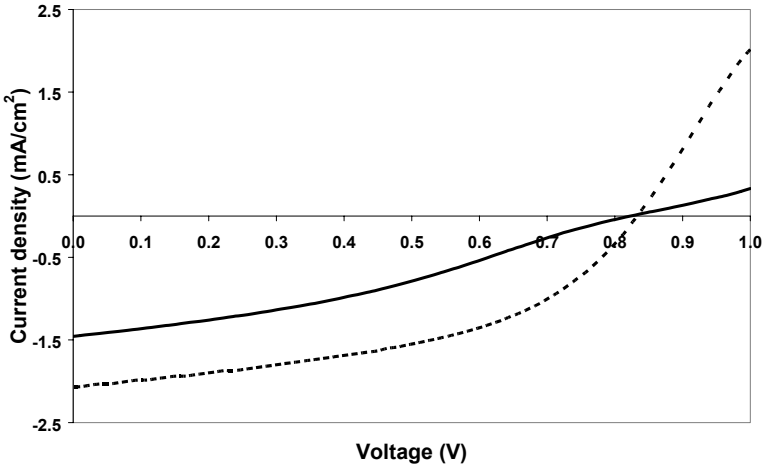

Fig. 1: I-V curves for control (solid) and lithium modified (dashed) ITO/mesoporous-TiO_2/MEH-PPV/Au devices tested under 0.8 sun AM1.5 simulated solar illumination.

The lithium concentration was optimized by varying the concentration of $Li[CF_3SO_2]_2N$ in the soaking solution from ≈4 mg/ml to 80 mg/ml (≈15 mM to 300 mM). Figures 2 and 3 show the variation of the device performance parameters (J_{sc}, V_{oc}, FF and η_{max}) with the concentration of the soaking solution. The J_{sc} and FF increase with increasing salt concentration, before reaching a plateau at approximately 25 mg/ml. The V_{oc} also increases slightly with increasing $Li[CF_3SO_2]_2N$ concentration, but begins to decrease for concentrations above 25 mg/ml, leading to an optimum efficiency at 25 mg/ml. The peak efficiency reached for these devices was less than the highest reported value above because a different Ti-Nanoxide paste was used, which may have had a lower degree of crystallinity.

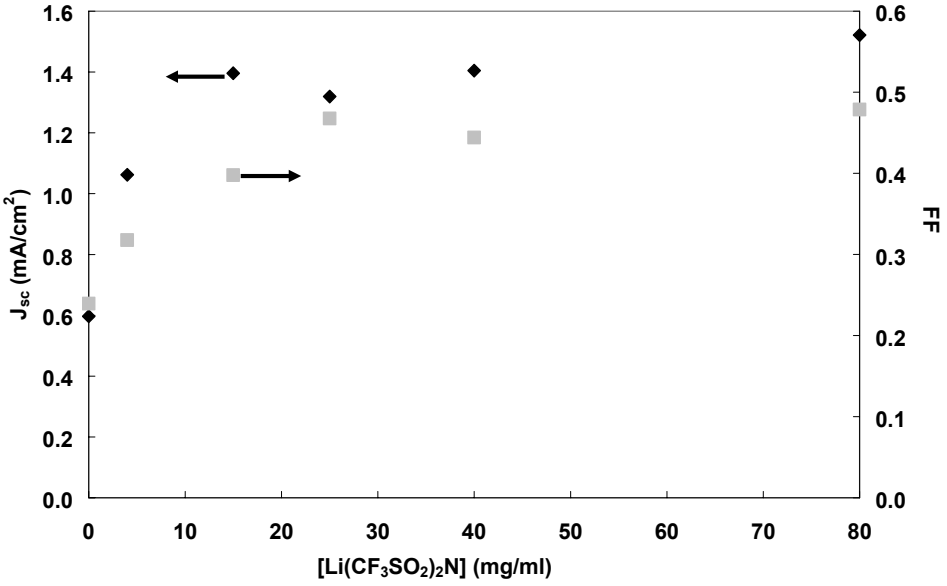

Fig. 2: Variation of J_{sc} (black diamonds) and FF (grey squares) with concentration of $Li[CF_3SO_2]_2N$ in the soaking solution. Control devices are shown at a soaking solution concentration of 0 mg/ml, but were actually un-soaked.

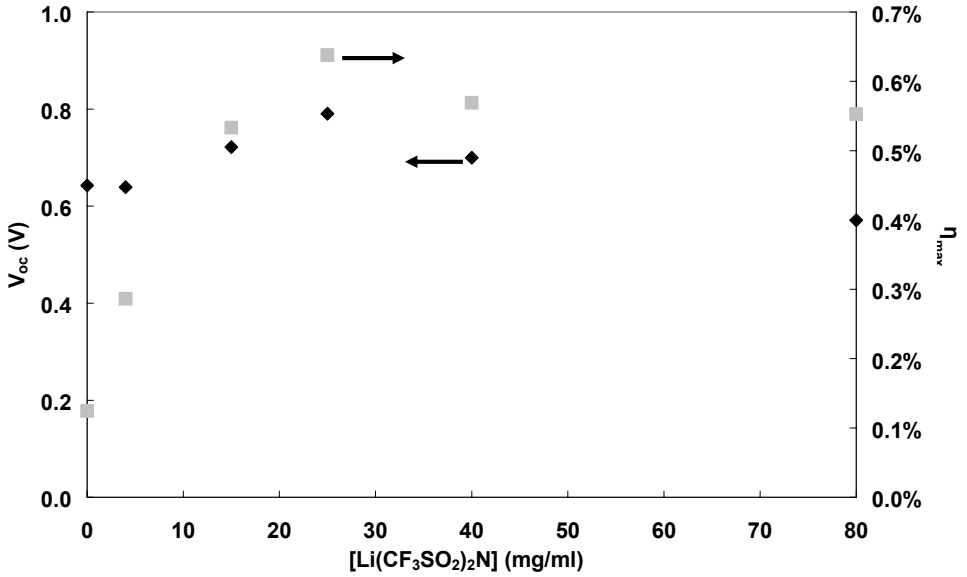

Fig. 3: Variation of V_{oc} (black diamonds) and η_{max} (grey squares) with concentration of $Li[CF_3SO_2]_2N$ in the soaking solution. Control devices are shown at a soaking solution concentration of 0 mg/ml, but were actually un-soaked.

3.1.2. Dense TiO_2 devices – interfacial modification

Figure 4 shows the I-V behaviour of devices containing a dense TiO_2 layer in place of the mesoporous TiO_2 layer, made by spin-coating and sintering a Ti-peroxide solution, both with and without interfacial $Li[CF_3SO_2]_2N$ modification. The modified devices show an increase in fill factor but no increase in J_{sc}, in contrast to similarly modified devices made with a porous TiO_2 layer. The V_{oc} also decreases slightly, with the net result that the η_{max} of modified and control devices is the same.

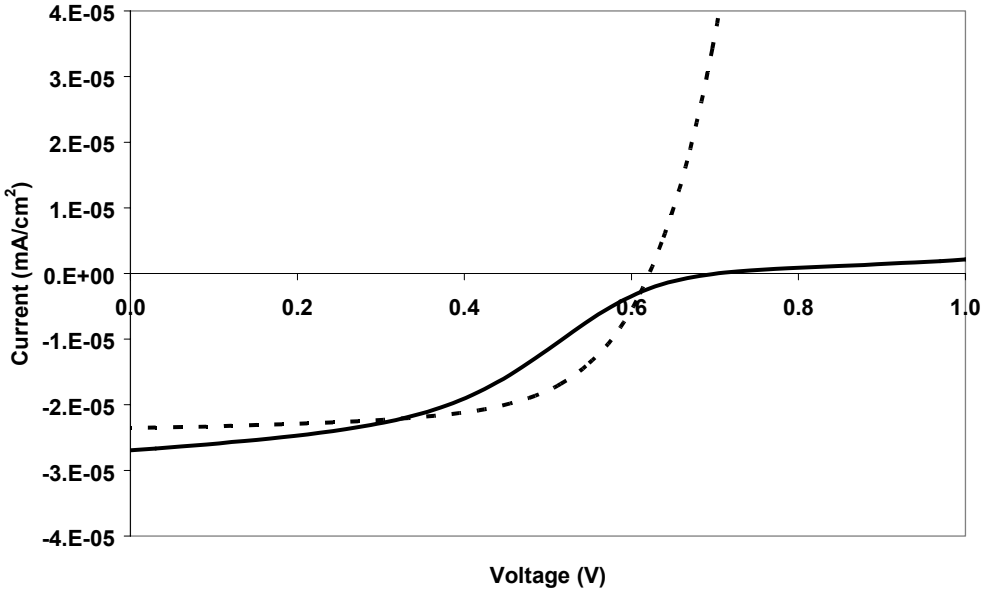

Fig. 4: I-V behaviour of ITO/Dense-TiO_2/MEH-PPV/Au devices, both with (dashed line) and without (solid line) interfacial $Li[CF_3SO_2]_2N$ modification, tested under 0.8 sun AM1.5 simulated solar illumination.

3.1.3. Mesoporous TiO_2 – polymer modification

In an attempt to determine the mechanism behind the device performance enhancement reported above for mesoporous TiO_2 devices, a small amount of $Li[CF_3SO_2]_2N$ dissolved in tBP was added to the polymer layer of some devices. Figure 5 shows the I-V behaviour of a control device compared with a device made with 0.13 mg/ml $Li[CF_3SO_2]_2N$ in the polymer spin-coating solution. The $Li[CF_3SO_2]_2N$ was first dissolved in tBP, which was present in the spin-coating solution at a concentration of 1:60 by volume. Both devices were of the type ITO/mesoporous-TiO_2/MEH-PPV/Au. As in the case of the dense TiO_2 devices, the fill factor of the modified device is enhanced relative to the control device, but the short-circuit current is slightly lower than the control device. The V_{oc} is unaffected within the error of the experiment, and the η_{max} is slightly increased in the modified device.

Figures 6 and 7 show the variation in the device performance parameters as a function of the concentration of $Li[CF_3SO_2]_2N$ in the polymer spin-coating solution. It is clear that adding neat tBP to the spin-coating solution reduces the J_{sc} and V_{oc} slightly, but adding a small amount of $Li[CF_3SO_2]_2N$/tBP solution has very little effect on either. The fill factor is improved slightly on addition of either neat tBP or $Li[CF_3SO_2]_2N$/tBP solution. The optimum concentration of $Li[CF_3SO_2]_2N$ is 0.13 mg/ml, which gives a η_{max} of 0.42 % relative to 0.33 % for the control device.

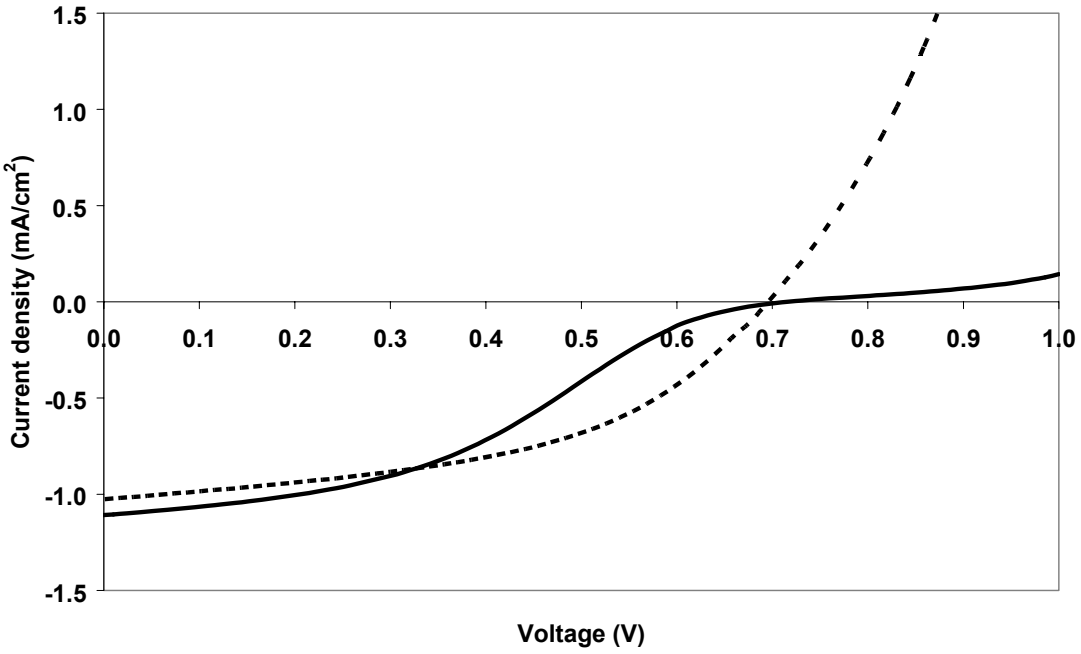

Fig. 5: I-V behaviour of devices of the type ITO/mesoporous-TiO_2/MEH-PPV/Au without (solid line) and with (dashed line) $Li[CF_3SO_2]_2N$/tBP in the polymer spin-coating solution. The concentrations of $Li[CF_3SO_2]_2N$ and tBP in the spin-coating solution were 0.13 mg/ml and 1:60 by volume, respectively.

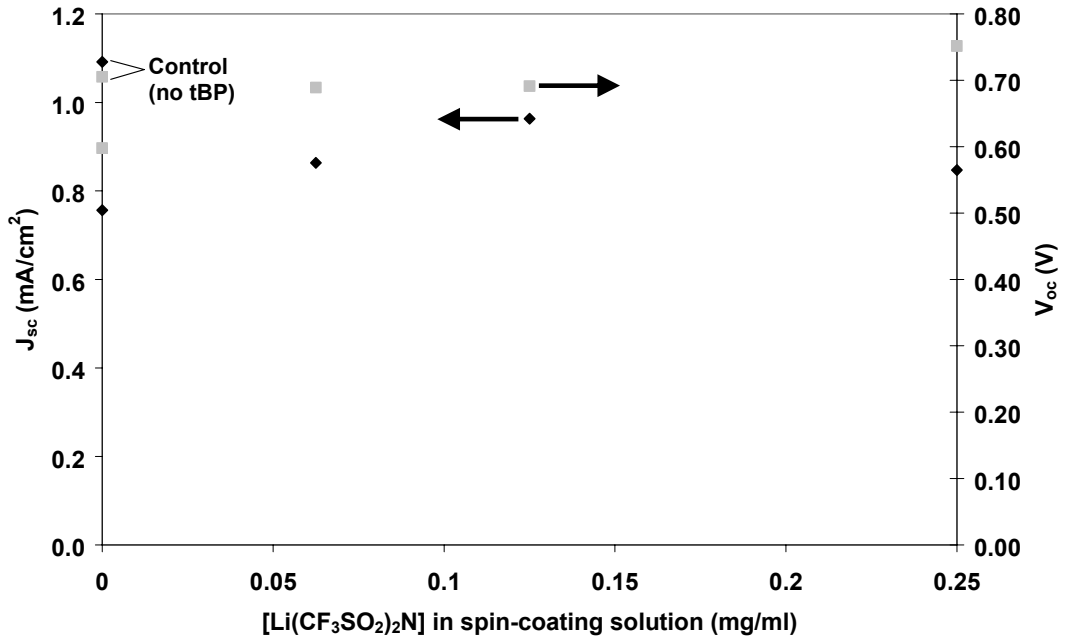

Fig. 6: J_{sc} (black diamonds) and V_{oc} (grey squares) vs. concentration of $Li[CF_3SO_2]_2N$ in the polymer spin-coating solution. The concentration of tBP was 1:60 by volume for all samples except the control samples, which are indicated.

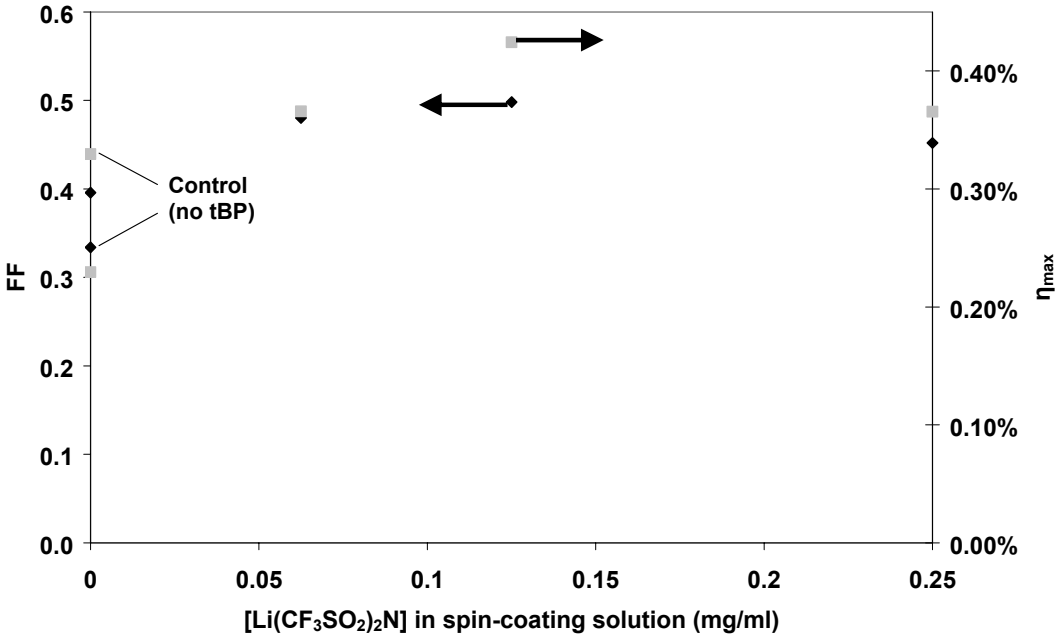

Fig. 7: Fill factor (black diamonds) and η_{max} (grey squares) vs. concentration of $Li[CF_3SO_2]_2N$ in the spin-coating solution. The concentration of tBP was 1:60 by volume for all samples except the control samples, which are indicated.

3.2. Chemical profiling – SIMS

Secondary ion mass spectroscopy depth profiles were obtained to determine the distribution of Li throughout the TiO_2 layer in interfacial Li modified devices. Figure 8 shows the amount of Li and Ti detected vs. time for two ITO/TiO_2 substrates which have been soaked in different concentrations of $Li[CF_3SO_2]_2N$/tBP solution. The variation of the sputtering rate over time makes it impossible to convert measurement time to depth directly. However, the depth of the crater left after depth profiling was 675 nm, which means that the profile extends more than half way through the TiO_2 layer. It is clear that increasing the concentration of the $Li[CF_3SO_2]_2N$/tBP soaking solution causes an increase in the amount of Li present throughout the TiO_2 layer, not just at the top surface. This is believed to be due to solution penetration into the pores in the mesoporous TiO_2 layer. The Li concentration increased by a factor of 3 for an order of magnitude increase in $Li[CF_3SO_2]_2N$ concentration in the soaking solution. The signal due to titanium is included to confirm that changes in the measured Li concentration are not due to a difference in the sputter rate between the two samples.

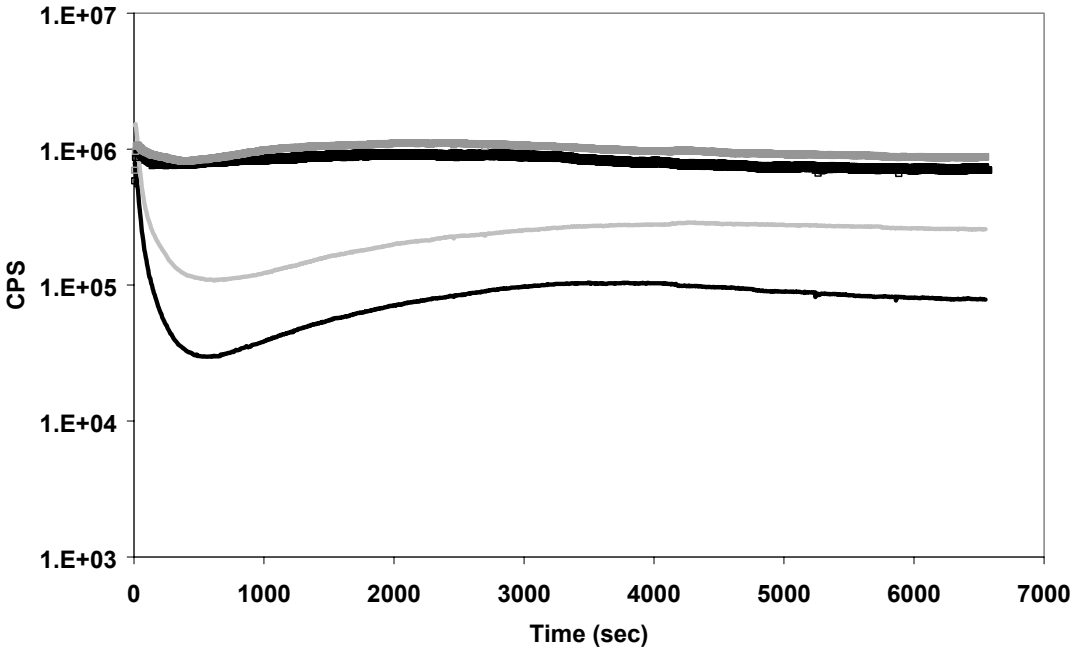

Fig. 8: Secondary ion mass spectroscopy signal (counts per second) vs. time, representing a depth profile of Li through the TiO_2 layer of two lithium modified ITO/TiO_2 substrates. The thin black and grey lines show the Li signal for the 4 mg/ml $Li[CF_3SO_2]_2N$/tBP soaked substrate and the 40 mg/ml $Li[CF_3SO_2]_2N$/tBP soaked substrate, respectively. The larger CPS for the latter indicates that there are more lithium ions present. The thick black and grey lines give the Ti signal for the 4 mg/ml and 40 mg/ml soaked substrates, respectively.

3.3. External quantum efficiency measurements

Figure 9 shows the external quantum efficiency (EQE) and normalized EQE spectra of interfacial Li modified and control devices made with mesoporous TiO_2. The maximum EQE value of 12% for the control device compares well with the value for similar devices reported in literature.[12, 13] The maximum EQE of the lithium-modified device is a factor of 1.9 larger than that for the control device. The spectra are qualitatively similar, as emphasized by the normalized EQE spectra, indicating that there is no shift in the onset of photocurrent generation.

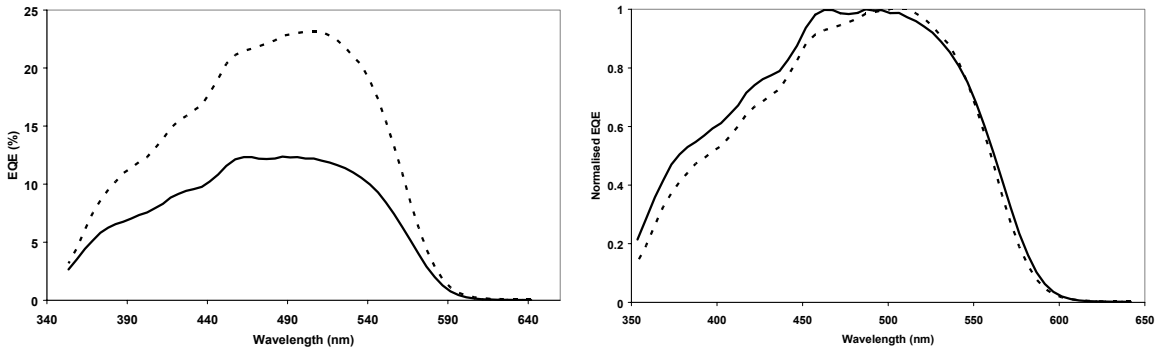

(a) (b)

Fig. 9: External quantum efficiency spectra for devices made with mesoporous TiO_2 without (solid line) and with (dashed line) interfacial lithium modification, before (a) and after (b) normalization.

4. DISCUSSION

The I-V behaviour of lithium modified devices seems to depend sensitively on the location of lithium within the device. This has already been observed by Kuang *et. al.*[10] for DSSC's. Lithium-modified mesoporous-TiO_2 devices, which have lithium throughout the TiO_2 layer, as confirmed by SIMS measurements, exhibit an increase in current and fill factor, resulting in a two-fold increase in device efficiency. When the lithium is added instead to the polymer layer of the device, the fill factor is increased (by a smaller factor) but the current is not, resulting in a much smaller improvement in device performance. When a device made with a dense TiO_2 layer is subjected to interfacial lithium modification, the fill factor is again improved, but the current is still unaffected and the V_{oc} is reduced slightly, with no net increase in device efficiency. In all three cases (polymer Li modification and interfacial Li modification of dense and porous TiO_2) $Li[CF_3SO_2]_2N$ is present at the interface between the two layers. This might mean that the fill factor is improved by the presence of lithium at the TiO_2/MEH-PPV interface, possibly by a charge screening or dipole effect which reduces recombination. The increase in current on the other hand cannot be due to an increased hole mobility in the polymer layer as it is not observed in the polymer Li modified devices. The fact that we have observed no change in V_{oc} following interfacial lithium modification of mesoporous TiO_2 devices, and that there is no red-shift in the onset of the EQE spectrum following interfacial lithium modification, indicates that increased injection from vibrationally-relaxed excited states due to lowering of the TiO_2 conduction band by adsorbed lithium ions, as observed by Kelly *et. al.* for DSSC's with Li ions in the electrolyte,[1] is not responsible for the increased current in our devices. This is not unexpected, since increasing the already substantial energy offset of 1.2 eV[14] between the LUMO of MEH-PPV and the conduction band (CB) of TiO_2 is not expected to make more TiO_2 CB energy levels available for exciton dissociation. Kruger *et. al.* reported that the addition of tBP and $Li[CF_3SO_2]_2N$ to the spin-coating solution of the polymer spiro-MeOTAD in a solid-state DSSC led to a dramatic increase in device performance, mainly due to an increase in photocurrent.[3] Through a combination of I-V and transient absorption spectroscopy measurements, they determined that both tBP and $Li[CF_3SO_2]_2N$ reduced the rate of interfacial recombination, which was attributed to changes in the space charge layer at the interface and a charge screening effect in the hole-conductor layer. It is unlikely that the same mechanism is responsible for the increased current in the lithium-modified mesoporous-TiO_2 devices examined here, as the current increase is not seen when $Li[CF_3SO_2]_2N$ is added to the polymer layer, nor is it seen for dense TiO_2 devices, as would be expected if it were a purely interfacial effect. A possible mechanism for the current enhancement is that there is not conformal contact between the polymer and TiO_2 in the case of the rough interface between MEH-PPV and the porous TiO_2 layer, and that the presence of $Li[CF_3SO_2]_2N$ at this interface improves electrical contact between the two layers by either improving contact directly (better polymer penetration into the pores) or mediating the interaction of the two layers. Alternatively, it might be due to 'doping' of the entire TiO_2 layer, leading to an increase in TiO_2 conductivity. This increase in conductivity has been confirmed by photoconductivity experiments which show a three-fold increase in TiO_2 conductivity following interfacial lithium modification of the mesoporous TiO_2 layer.[15] While it has been shown that, for DSSC's, changes in the electron diffusion coefficient following lithium intercalation have no effect on photovoltaic characteristics of a device,[2] the same has not been proven for polymer/TiO_2 solar cells, which have a different space-charge distribution under illumination relative to DSSC's.[3]

5. CONCLUSION

Polymer/TiO_2 photovoltaic devices were modified with $Li[CF_3SO_2]_2N$ dissolved in 4-*tert*-butyl pyridine. When these were added to the polymer layer, or at the polymer/TiO_2 interface, the fill factor of devices increased but the short-circuit current and open-circuit voltage were unaffected. When present throughout the (porous) TiO_2 layer, both the fill factor and short-circuit current increased by 40%, leading to a two-fold increase in device efficiency. The highest device performance obtained was 1.05 %, a world-leading efficiency for MEH-PPV/TiO_2 devices. The increase in fill factor might be attributed to charge screening effects, while the increase in current for lithium modified mesoporous-TiO_2 devices could be attributed to the observed three-fold increase in the conductivity of the TiO_2 layer, leading to improved electron transport and charge screening. The increase in current could also be due to a possible improvement in contact between the polymer and TiO_2 layers. Future experiments will look at the effect of varying the cation and anion, to determine the effects of properties such as ionic radius and charge-to-radius ratio on device performance.

Further SIMS experiments will be used to correlate changes in device performance with spatial distribution of cations throughout the device.

6. ACKNOWLEDGEMENTS

Financial support from the Toppan Printing Company and Engineering and Science Research Council (UK) is gratefully acknowledged. DARB is a Rhodes Scholar. We would also like to thank Matt Kilburn for performing the SIMS measurements, Hannah Smith for help with the EQE measurements, Bimlesh Lochab for purifying tBP, and Victor Burlakov and Christopher Martin for helpful discussions.

7. REFERENCES

1. C. A. Kelly, F. Farzad, D. W. Thompson, J. M. Stipkala, and G. J. Meyer, "Cation-controlled interfacial charge injection in sensitized nanocrystalline TiO2", *Langmuir*, **15**, p. 7047-7054, 1999.
2. N. Kopidakis, K. D. Benkstein, J. van de Lagemaat, and A. J. Frank, "Transport-limited recombination of photocarriers in dye- sensitized nanocrystalline TiO2 solar cells", *J. Phys. Chem. B*, **107**, p. 11307-11315, 2003.
3. J. Kruger, R. Plass, L. Cevey, M. Piccirelli, M. Gratzel, and U. Bach, "High efficiency solid-state photovoltaic device due to inhibition of interface charge recombination", *Appl. Phys. Lett.*, **79**, p. 2085-2087, 2001.
4. H. J. Snaith, S. M. Zakeeruddin, L. Schmidt-Mende, C. Klein, and M. Gratzel, "Ion-coordinating sensitizer in solid-state hybrid solar cells", *Angew. Chem., Int. Ed.*, **44**, p. 6413-6417, 2005.
5. K. Murakoshi, R. Kogure, Y. Wada, and S. Yanagida, "Fabrication of solid-state dye-sensitized TiO2 solar cells combined with polypyrrole", *Sol. Energy Mater. Sol. Cells*, **55**, p. 113-125, 1998.
6. S. A. Haque, T. Park, C. Xu, S. Koops, N. Schulte, R. J. Potter, A. B. Holmes, and J. R. Durrant, "Interface engineering for solid-state dye-sensitized nanocrystalline solar cells: The use of ion-solvating hole- transporting polymers", *Adv. Funct. Mater.*, **14**, p. 435-440, 2004.
7. T. Park, S. A. Haque, R. J. Potter, A. B. Holmes, and J. R. Durrant, "A supramolecular approach to lithium ion solvation at nanostructured dye sensitised inorganic/organic heterojunctions", *Chem. Commun.*, 2878-2879, 2003.
8. U. Bach, D. Lupo, P. Comte, J. E. Moser, F. Weissortel, J. Salbeck, H. Spreitzer, and M. Gratzel, "Solid-state dye-sensitized mesoporous TiO2 solar cells with high photon-to-electron conversion efficiencies", *Nature*, **395**, p. 583-585, 1998.
9. K. Peter, H. Wietasch, B. Peng, and M. Thelakkat, "Dual-functional materials for interface modifications in solid-state dye-sensitised TiO2 solar cells", *Appl. Phys. A-Mater. Sci. Process.*, **79**, p. 65-71, 2004.
10. D. B. Kuang, C. Klein, H. J. Snaith, J. E. Moser, R. Humphry-Baker, P. Comte, S. M. Zakeeruddin, and M. Gratzel, "Ion coordinating sensitizer for high efficiency mesoscopic dye-sensitized solar cells: Influence of lithium ions on the photovoltaic performance of liquid and solid-state cells", *Nano Lett.*, **6**, p. 769-773, 2006.
11. Z. Xie, B. M. Henry, K. R. Kirov, H. E. Smith, A. Barkhouse, C. R. M. Grovenor, H. E. Assender, G. A. D. Briggs, G. R. Webster, P. L. Burn, M. Kano, and Y. Tsukahara, "Study of the effect of changing the microstructure of titania layers on composite solar cell performance", *Thin Solid Films*, **511**, p. 523-528, 2006.
12. L. H. Slooff, J. M. Kroon, J. Loos, M. M. Koetse, and J. Sweelssen, "Influence of the relative humidity on the performance of polymer/TiO2 photovoltaic cells", *Adv. Funct. Mater.*, **15**, p. 689-694, 2005.
13. K. M. Coakley and M. D. McGehee, "Photovoltaic cells made from conjugated polymers infiltrated into mesoporous titania", *Appl. Phys. Lett.*, **83**, p. 3380-3382, 2003.
14. A. J. Breeze, Z. Schlesinger, S. A. Carter, and P. J. Brock, "Charge transport in TiO2/MEH-PPV polymer photovoltaics", *Phys. Rev. B*, **6412**, p. 2001.
15. Z. Xie, B. M. Henry, K. R. Kirov, D. A. R. Barkhouse, V. M. Burlakov, H. E. Smith, C. R. M. Grovenor, H. E. Assender, G. A. D. Briggs, M. Kano, and Y. Tsukahara, "Correlation between photoconductivity in nanocrystalline titania and short circuit current transients in MEH-PPV/titania solar cells", *Nanotechnology*, In Submission.